Influence of substrate temperature on structural and optical properties of RF sputtered ZnMnO thin films

© Parisa Pashaei*+, Nihan Akin*+¶, U. Ceren Baskose*+, M. Kemal Ozturk*+, Mehmet Cakmak*+, Suleyman Ozcelik*+¶¶

* Photonics Application and Research Center, Gazi University, 06500 Ankara, Turkey
+ Department of Physics, Gazi University, 06500 Ankara, Turkey

(Получена 11 сентября 2014 г. Принята к печати 25 сентября 2014 г.)

The ZnMnO thin films were deposited on glass substrates by radio frequency magnetron sputtering method. The properties of ZnMnO thin films were investigated by high-resolution x-ray diffractometer (HRXRD), atomic force microscopy (AFM), UV-Vis spectrometer and room temperature photoluminescence (PL), under the influence of substrate temperature. The substrate temperature was varied from 300, 400 and 500°C. With increasing the substrate temperature, the structure of the films changed from cubicto hexagonal. The cubic ZnMnO thin films grown along [210] direction, while the hexagonal ones grown along [002] direction. The changes in surface morphology provided a proof on the structural transition. Also, decrease and increase of optical band gap is associated with cubic or hexagonal structure of the films.

1. Introduction

As a wide bandgap (3.37 eV) semiconductor, ZnO is favored material and has been commonly investigated invariousdevicessuch as gas sensors, thin-film transistors, surface acoustic wave devices, pyroelectric devices, varistors and transparent electrodes [1–3]. Furthermore, ZnO is an attractive material for shortwavelength optoelectronic applications because of its large exciton binding energy (60 meV) and the possibility of tuning the band gap by doping or alloying with some metals like aluminum (Al), boron (B), gallium (Ga), indium (In) andmagnesium (Mg) etc. Al is widely used as dopants in most researches based on ZnO [4–6], but if itpresents a high reactivity, it may lead to oxidation during the growth of the films. Therefore, as an alternative, it is possible to use of Gawhich is less reactive and more resistant to oxidation compared to Al [7]. The choice of doping materials is very important for the applications of theZnO thin films, for example, Mg is an ideal candidate doped material for ZnO based UV photodetectors [8–10] because of its composition is effective in shifting to short wavelength of absorption edge of the films.

Until now, a few groups investigated in dopingor alloying with some transition metals like cadmium (Cd), molybdenum (Mo) and manganese (Mn) [11–14]. Among all transition metals Mn is more appropriate, since its large thermal equilibrium solubility (13 at%) and nearly the same ionic radii (0.66 Å) as compared to Zn (0.60 Å). Various growth techniques, including molecular beam epitaxy [15], spray pyrolysis [16], metal organic chemical vapor deposition [17], radio frequency (RF) magnetron sputtering [18], sol-gel method [19], and pulsed laser deposition [20], have been employed to deposition of ZnMnO thin films. Among these processes used to prepare ZnMnO thin films, magnetron sputtering is a suitable technique because of its flexibility in the control of composition and microstructure. The effect of deposition properties such as substrate temperature, grow rate, pressure, ambient gasis very important during deposition in radio frequency magnetron sputtering process.

Recently, much attention has been paid to ferromagnetic properties of the ZnMnO thin films because of their potential spintronic sapplications for diluted magnetic semiconductors (DMSs) with Curie temperatures (T_C) above room temperature [18–22]. However, it is important to investigate the other properties such as structuraland optical properties of the films are alsonecessary in applications of devices. In literature, the effect of substrate temperature on structural and optical properties of the RF sputtered ZnMnO thin films on glass substrate has not been studied in detail yet. Therefore, the main purpose of presented work was to investigate the structural, surface morphological and optical properties of the films. ZnMnO thin films deposited on glass substrates by using RF magnetron sputtering and influence of substrate temperature on the structural, morphological and optical properties of the films was investigated by high-resolution x-ray diffractometer (HRXRD), atomic force microscopy (AFM), UV-Vis spectrometer and room temperature photoluminescence (PL) respectively.

2. Experimental procedure

The ZnMnO thin films deposited on glass substrates by radio frequency (RF) magnetron sputtering system (BESTEC) using a ceramic target prepared from high purity ZnO powder and mixed with 36 wt% MnO_2 powder. Substrates were carefully cleaned by ethanol and dried under flowing N_2 gas. The chamber was evacuated to a base pressure of about 2.9×10^{-8} mbar. High purity (99.999%) Ar was introduced into the chamber and mea-

¶ E-mail: nihanakinn@gmail.com
¶¶ E-mail: sozcelik@gazi.edu.tr

HRXRD results of ZnMnO thin films at various substrate temperatures

Substrate temperature (°C)	Structure	(hkl)	2θ (deg.)	d (Å)	FWHM (deg.)	Grain Size (nm)	c_{film} (Å)
300	Cubic	210	41.52	2.1731	0.506	28.97	4.8594
400	Hexagonal	002	34.33	2.6100	0.341	42.08	5.2201
500	Hexagonal	002	34.39	2.6056	0.327	43.89	5.2113

sured by mass flow controllers for a total flow rate fixed at 18 sccm. In order to clean the target surface, a pre-sputtering process was employed for 20 min in Ar (Argon) gas before deposition films. The substrate temperatures were fixed at 300, 400 and 500°C, respectively. Sputtering pressure (P_S) was kept at 5.4×10^{-3} mbar during the deposition. RF power was set at 250 W and the distance between target and substrate was about 35 mm for the all samples. The growth rate of the films was 1.7–2.0 A/sec and the total thickness was about 200–300 nm. Thickness of the deposited films was measured a thickness meter by insuite.

After the deposition, the thickness of the films was measured with a stylus type profile meter (Dektak 150). The structure and crystalline quality of the films were detected with high-resolution x-ray diffractometer (D8 Discover, Bruker) using Cu$K_{\alpha 1}$ (1.540 Å) radiation, and a 4-crystaled Ge(220) symmetric monochromator. The surface morphology of the films was characterized with high performance atomic force microscope (hpAFM, Nano-Magnetics Instruments) by using dynamic mode scanning. The optical transmittance measurements were performedby UV-Vis spectrometer (Lambda 2S, Perkin Elmer) at RT in the range of 200–1100 nm. Optical band gap of the films were performed by room temperature PL measurements (HORIBA Jobin Yvon) by using a 50 mW HeCd laser ($\lambda = 325$ nm) which is an excitation light source.

3. Results and discussion

3.1. Structural properties

ZnMnO crystallizes in two structures: hexagonal wurtzite (at ambient pressure and temperature) and cubic zinc blend. It is known that the hexagonal structure is the most stable one. However, ZnMnO thin films can grow in mixed phase (cubic + hexagonal) depending on the deposition method and conditions, especially according to the doping or alloying. To avoid mixed phase, the growth system and the films should be prepared very carefully.

Fig. 1 shows HRXRD patterns of RF sputtered ZnMnO thin films on glass substrates at various substrate temperatures. As it clear from the figure, the crystal structure of the films is changed by increasing the substrate temperature. At 300°C, (210) peak is observed at 41.417°, indicating that the film is in cubic structure. At 400°C, it is shown that the film structure changes to hexagonal structure due to (002) peak is observed at 34.432°. The (002) peak becomes more intense and sharper at 500°C, as well as it is seen that full width half of maximum (FWHM) values listed in Table. Increasing in intensity and sharper FWHM reveal improvement of the crystallization of ZnMnO thin films.

The grain size of the films were calculated from the FWHM values using the Scherrer's formula [23]:

$$D = K\lambda / B \cos\theta. \quad (1)$$

Where, D is the grain size, K is the constant (equal 0.9 assuming that the particles are spherical), λ is the wavelength of x-ray (= 1.540598 Å), B is the line width (FWHM) and θ is the Bragg angle. The grain size increased from 28.97 to 43.89 nm and FWHM decreased from 0.506 to 0.327 with increasing the substrate temperature. The lattice parameters $a_{\text{film}} = b_{\text{film}} = c_{\text{film}}$ of cubic and c_{film} (because of c-oriented) of hexagonal structure were found to agree well with the bulk ($c_{\text{bulk}} = 4.87100$ as JCPDS card No 01-076-1364 for cubic structure and $c_{\text{bulk}} = 5.20661$ as JCPDS card No 00-036-1451 for hexagonal structure) values, as seen in table. These results show that Mn ions tended to substitute for Zn sites with changing structure of ZnO at substrate temperature of 300°C, but increasing the substrate temperature, Mn did not affect the structure of ZnO and Mn ions substitute for Zn sites in the film. Additionally, the c-axis is a strong preferred orientation at substrate temperature of 500°C. This means that the ZnMnO thin film deposited at 500°C appears to have the best crystallinity. The similar results have been obtained in literature. Gopalakrishnan et al. [24] prepared ZnMnO thin

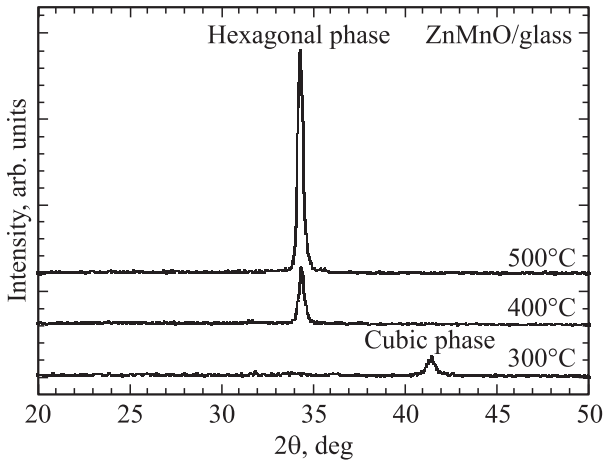

Figure 1. HRXRD patterns of ZnMnO thin films.

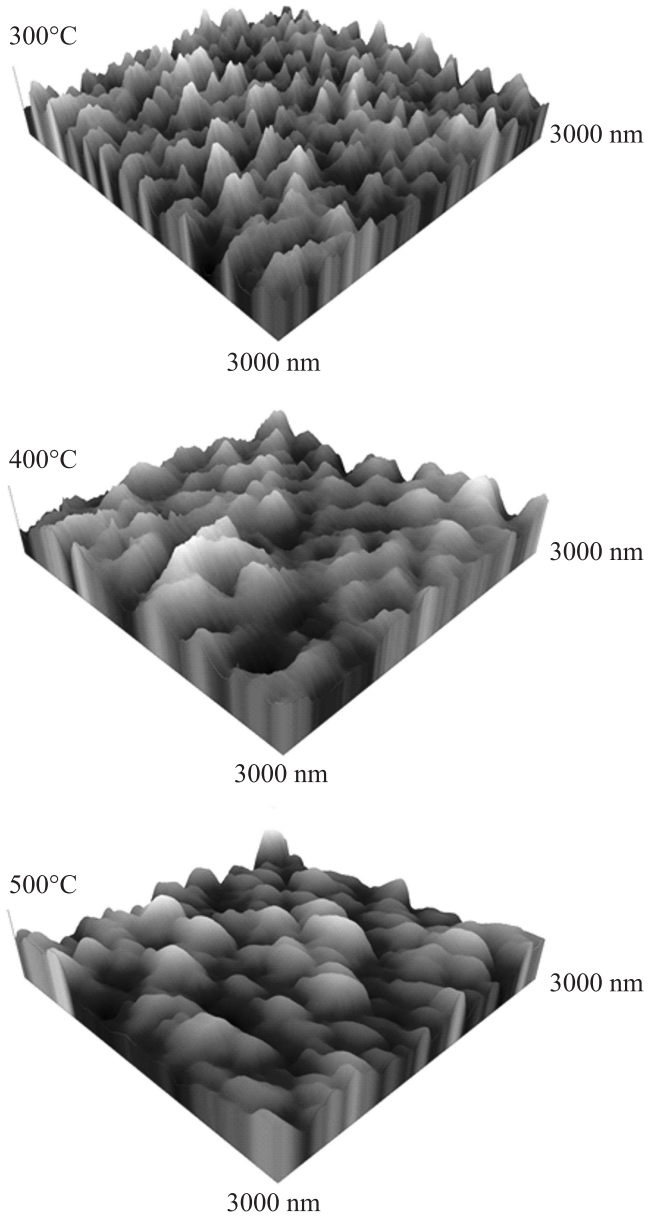

Figure 2. 3D AFM images of ZnMnO thin films.

films on Si substrates by using RF magnetron sputtering at substrate temperature of 450°C in order to investigate the effect of oxygen vacancies on ferromagnetism (FM) in the films. Their x-ray diffraction researches revealed that the films were strongly oriented along the (002) orientation that correspond to the hexagonal wurtzite structure and free from the formation of any secondary phases, as the same our results substrate temperature of above 400°C.

3.2. Surface morphology

Fig. 2 shows three-dimensional (3D) AFM images with $3 \times 3\,\mu m^2$ scan area of RF sputtered ZnMnO thin films on glass substrates at different substrate temperatures. The root mean square (RMS) values of the surface roughness of the films were measured to understand the surface uniformity of the films at nanoscale. It was found that the films deposited at various substrate temperatures had different surface roughness. The RMS values of 1.09, 1.61 and 4.66 nm were determined for the surface roughness of the samples at substrate temperature of 300, 400 and 500°C, respectively. The increase of RMS values is associated with the increase of grain size, as can be seen in Fig. 2.

Observation of the phase transitionsfrom the AFM imagesis another important result which is consistent with the trend observed from HRXRD results. It was seen that the surface structure of ZnMnO thin films is pyramidal shaped crystallites at substrate temperature of 300°C, is prism shaped crystallites at substrate temperature of 400 and 500°C. Pyramidal shaped crystal is a typical form of cubic crystallites and prism shaped crystallites of hexagonal ones [25]. At higher substrate temperature, the shape of the crystallites is well defined at prism geometry. Also, the surface morphology is quite uniform at nanoscale. The AFM results indicate that surface morphology of the ZnMnO thin films is largely affected by substrate temperature.

3.3. Optical properties

Fig. 3 showsthe transmittance spectra as a function of wavelength in the range from 200−1100 nm for the bare glass substrate and RF sputtered ZnMnO thin films on glass substrates. The transmittance of the films changed according to the substrate temperature. The band gap is estimated from absorption edge of the films. The optical absorption coefficient α can be derived using the formula [26]:

$$\alpha h\nu = A(h\nu - E_g)^m. \qquad (2)$$

Where, A is a constant, h is Planck's constant, ν is the frequency of the incident radiation, E_g is the energy gap and m value is respectively 1/2 and 2 for direct and indirect

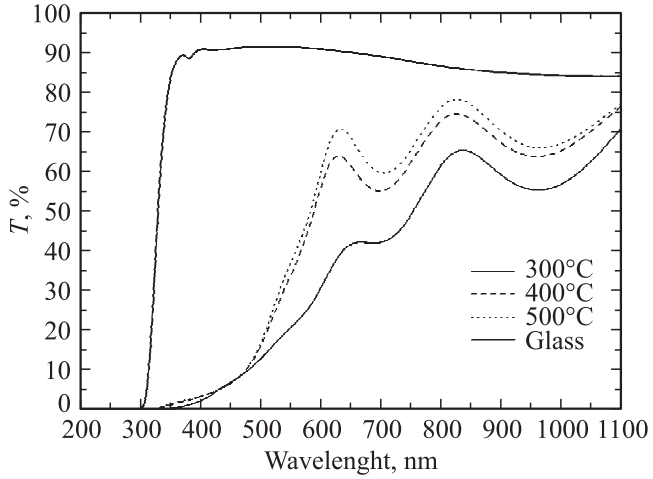

Figure 3. The transmission spectra of the bare glass substrate and ZnMnO thin films.

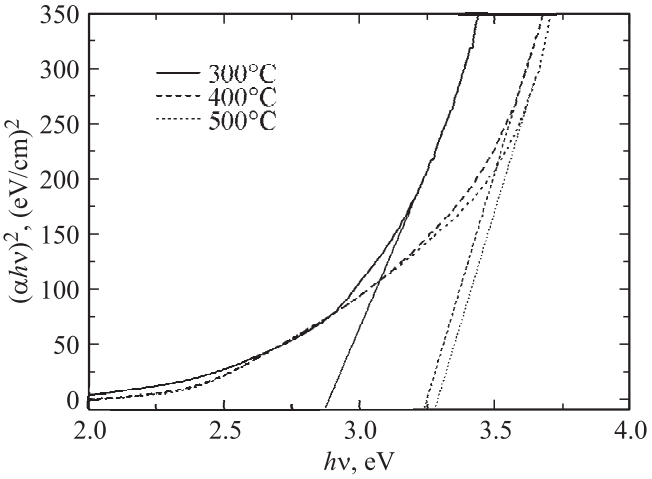

Figure 4. Plot of $(\alpha h\nu)^2$ against $h\nu$ of ZnMnO thin films.

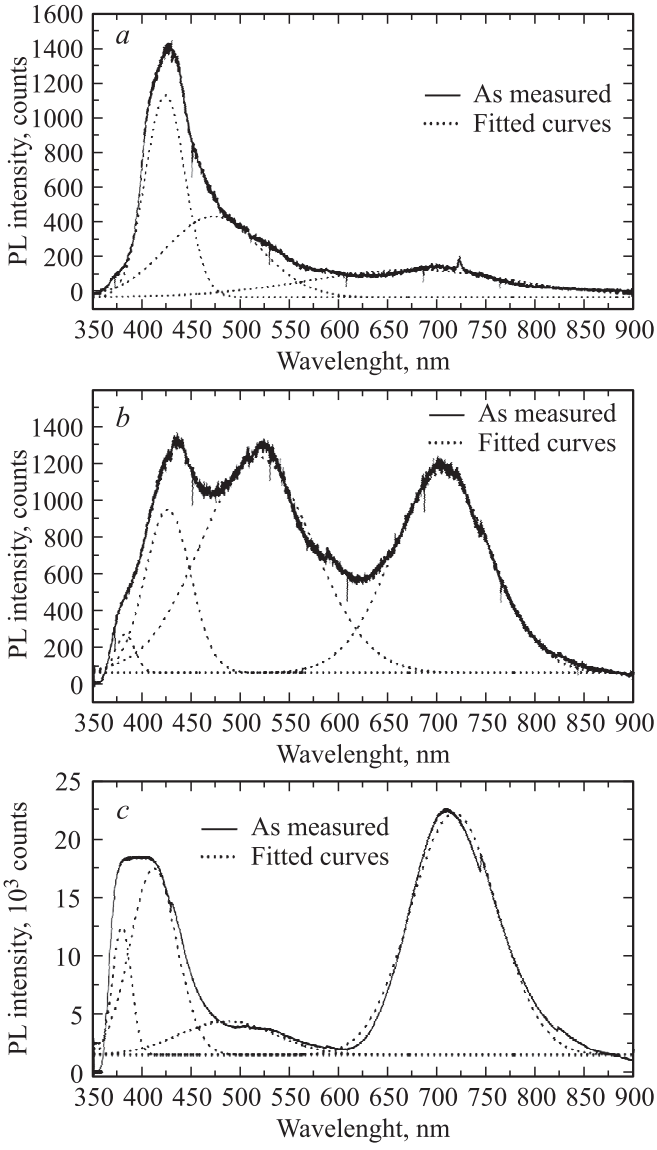

Figure 5. Room temperature PL spectrum (solid line) and Gaussian fitting (doted line) of ZnMnO thin films, °C. *a* — 300, *b* — 400, *c* — 500.

transitions. The Eg can be obtained by plotting $(\alpha h\nu)^m$ versus $h\nu$. The extrapolations of these plots on the energy axis give the energy band gaps.

Fig. 4 shows plot of $(\alpha h\nu)^2$ against $h\nu$ of the ZnMnO thin films. Optical band gaps of the films were found to be 2.88, 3.24 and 3.28 eV at substrate temperature of 300, 400 and 500°C, respectively. Baghdad at al. [27] noted that optical band gap value increases due to the Burstein–Moss effect. Yadav at al. [28] reported the band gap of Mn doped ZnO films increases lightly with incorporation of Mn at Zn site. The present study showed that optical band gap of the ZnMnO thin films were influenced by the crystalline structure. As it clear from the results, the cubic crystal structure of the films provided a lower band gap value than the hexagonal crystal structure of the films. Besides, increasing the substrate temperature of the films caused increasing the optical band gap for hexagonal structure.

Fig. 5 shows the room temperature PL spectrum and Gaussian fitting for RF sputtered ZnMnO thin films on glass substrates at substrate temperature of (*a*) 300, (*b*) 400 and (*c*) 500°C, respectively. The Gaussian analysis method of fitting multi-peaks was used to investigate the emission peaks of the films. Near band-edge (NBE) emission (band-to-band transition) peak at 2.93 eV (423 nm), 3.24 eV (382 nm), 3.27 eV (379 nm) was observed, respectively. It was found that the similar optical band gapof the films from the UV-Vis spectrometer results in this presented work.

Although there have been with strong UV and weak defect emission in cubic structure, the UV emission is much weaker compared to the defect emission in hexagonal structures. As known, the blue and green emission is attributed to oxygen vacancies (V_0) and zinc interstitials (Zn_i). The red emission attributed to defects of oxygen interstitials (O_i) [29,30]. In the light of this knowledge can be said that the green emission around 500 nm was observed in hexagonal ZnMnO thin films that was due to the oxygen vacancies in the structures. However, it is important that the intensity of the green emission peaks decreased with increasing the substrate temperature. This means that both HRXRD and PL results also support each other. The ZnMnO thin films deposited at 500°C appears to better crystallinity than lower substrate temperature.

4. Conclusion

ZnMnO thin films with different substrate temperature were successfully deposited on glass substrates by RF magnetron sputtering. Structural, morphological and optical properties of the obtained films were investigated. The structural transition from cubic to hexagonal phase was observed not only structural but also morphological and optical results. These results showed that the critical temperature for the structural transition of the RF sputtered ZnMnO thin films was betweenat substrate temperature of 300 and 400°C. The films prepared at substrate temperature of 500°C had the best crystallinity and highly oriented

along the (002) direction with the *c*-axis perpendicular to the substrate. The surface of the films was extremely flat and uniform at nanoscale. Optical band gap of the films was found to be influenced by the crystalline structure. The quality of the films is greatly affected by substrate temperature during deposition.

This work was supported by the Ministry of Development of TR under Project No 2011K120290.

References

[1] S. Masuda, K. Kitamura, Y. Okumura, S. Miyatake. J. Appl. Phys. **93**, 1624 (2003).
[2] D. Chu, T. Hamada, K. Kato, Y. Masuda. Phys. Status Solidi A, **206**, 718 (2009).
[3] S.S. Shinde, K.Y. Rajpure. J. Alloys Comp., **522**, 118 (2012).
[4] J.M. Kim, P. Thiyagarajan, S.W. Rhee. Thin Solid Films, **518**, 5860 (2010).
[5] N. Akin, S.S. Cetin, M. Cakmak, T. Memmedli, S. Ozcelik. J. Mater. Sci.: Mater. Electron., **24**, 5091 (2013).
[6] C. Guillen, J. Herrero. Phys. Status Solidi A, **206**, 1531 (2009).
[7] E. Fortunato, L. Raniero, L. Silva, A. Goncalves, A. Pimentel, P. Barquinha, H. Aguas, L. Pereira, G. Goncalves, I. Ferreira, E. Elangovan, R. Martins. Sol. Energy Mater. Sol. Cells, **92**, 1605 (2008).
[8] S. Han, D.Z. Shen, J.Y. Zhang, Y.M. Zhao, D.Y. Jiang, Z.G. Ju, D.X. Zhao, B. Yao. J. Alloys Comp., **485**, 794 (2009).
[9] K. Liu, M. Sakurai, M. Aono. Sensors, **10**, 8604 (2010).
[10] P. Kumar, H.K. Malik, A. Ghosh, R. Thangavel, K. Asokan. Appl. Phys. Lett., **102**, 221 903 (2013).
[11] F. Yakuphanoglu, S. Ilican, M. Caglar, Y. Caglar. Superlat. Microstr., **47**, 732 (2010).
[12] A. Boukhachem, B. Ouni, M. Karyaoui, A. Madani, R. Chtourou, M. Amlouk. Mater. Sci. Semicond. Proc., **15**, 282 (2012).
[13] X.Y. Li, H.J. Li, M. Yuan, Z.J. Wang, Z.Y. Zhou, R.B. Xu, J. Alloys Comp., **509**, 3025 (2011).
[14] H.K. Yadav, K. Sreenivas, V. Gupta. J. Appl. Phys., **99**, 083 507 (2006).
[15] H.J. Lin, D.Y. Lin, J.Z. Hong, C.S. Yang, C.M. Lin, C.F. Lin. Phys. Status Solidi C, **6**, 1468 (2009).
[16] A.U. Ubale, V.P. Deshpande. J. Alloys Comp., **500**, 138 (2010).
[17] W.M. Hlaingo, L.V. Saraf, M.H. Engelhard, V. Shutthanandan, L. Bergman, J. Huso, M.D. McCluskey. J. Appl. Phys., **105**, 013 715 (2009).
[18] C. Liu, F. Yun, B. Xiao, S.J. Cho, Y.T. Moon, H. Morkoc. J. Appl. Phys., **97**, 126 107 (2005).
[19] Y.M. Kim, M. Yoon, I.W. Park, Y.J. Park, J.H. Lyou. Sol. St. Commun., **129**, 175 (2004).
[20] J. Zhang, X.Z. Li, J. Shi, Y.F. Lu, D.J. Sellmyer. J. Phys.: Condens. Matter, **19**, 036 210 (2007).
[21] M.D. Mukadam, S.M. Yusuf. Physica B, **403**, 2602 (2008).
[22] S.W. Jung, S.J. An, G.C. Yi, C.U. Jung, S.I. Lee, S. Cho. Appl. Phys. Lett., **80**, 4561 (2002).
[23] H.P. Klug, L.E. Alexander. *X-Ray Diffraction Procedures* (Wiley, N.Y., 1974.)
[24] N. Gopalakrishnan, L. Balakrishnan, B. Srimathy, M. Senthil Kumar, T. Balasubramanian. Phys. Status Solidi A, **207**, 2180 (2010).
[25] R. Ramirez-Bon, N.C. Sandoval-Inda, F.J. Espinoza-Beltran, M. Sotelo-Lerma, O. Zelaya-Angel, C. Falcony. J. Phys.: Condens. Matter, **9**, 10 051(1997).
[26] J.I. Pankove. *Optical Process in Semiconductors* (Dover, N.Y., 1976).
[27] R. Baghdad, B. Kharroubi, A. Abdiche, M. Bousmaha, M.A. Bezzerrouk, A. Zeinert, M. El Marssi, K. Zellama. Superlat. Microstr., **52**, 711 (2012).
[28] H.K. Yadav, K. Sreenivas, V. Gupta. J. Appl. Phys., **99**, 083 507 (2006).
[29] W. Liu, X. Tang, Z. Tang. J. Appl. Phys., **114**, 123 911 (2013).
[30] A.B. Djurisic, Y.H. Leung. Small, **2**, 944 (2006).

Редактор Т.А. Полянская